ACS APPLIED MATERIALS & INTERFACES

Letter

Cite This: ACS Appl. Mater. Interfaces 2018, 10, 10607−10611

www.acsami.org

Structure of Ultrathin Native Oxides on III−Nitride Surfaces

J. Houston Dycus,[†] Kelsey J. Mirrielees,[†] Everett D. Grimley,[†] Ronny Kirste,[†,‡] Seiji Mita,[†,‡] Zlatko Sitar,[†,‡] Ramon Collazo,[†] Douglas L. Irving,[†] and James M. LeBeau*[,†]

[†]Department of Materials Science and Engineering, North Carolina State University, Raleigh, North Carolina 27695, United States

[‡]Adroit Materials, Inc., 2054 Kildaire Farm Road, Suite 205, Cary, North Carolina 27518, United States

Supporting Information

ABSTRACT: When pristine material surfaces are exposed to air, highly reactive broken bonds can promote the formation of surface oxides with structures and properties differing greatly from bulk. Determination of the oxide structure is often elusive through the use of indirect diffraction methods or techniques that probe only the outermost layer. As a result, surface oxides forming on widely used materials, such as group III-nitrides, have not been unambiguously resolved, even though critical properties can depend sensitively on their presence. In this study, aberration corrected scanning transmission electron microscopy reveals directly, and with depth dependence, the structure of ultrathin native oxides that form on AlN and GaN surfaces. Through atomic resolution imaging and spectroscopy, we show that the oxide layers are comprised of tetrahedra−octahedra cation−oxygen units, in an arrangement similar to bulk θ-Al_2O_3 and β-Ga_2O_3. By applying density functional theory, we show that the observed structures are more stable than previously proposed surface oxide models. We place the impact of these observations in the context of key III-nitride growth, device issues, and the recent discovery of two-dimensional nitrides.

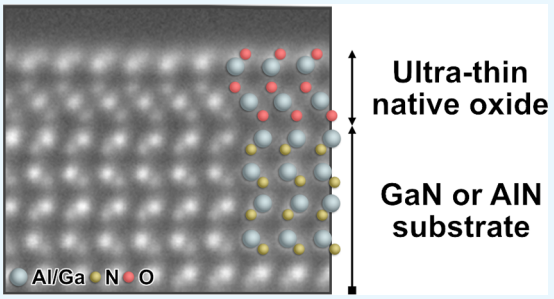

KEYWORDS: *ultrathin oxides, surface reconstructions, group III nitrides, scanning transmission electron microscopy, density functional theory*

Group III nitrides, such as GaN and AlN, are the bedrock of modern solid-state lighting. Further, they are of particular interest for high power devices because of their strong polarization fields that can confine carriers to heterointerfaces supplied via extrinsic doping or surface states.[1,2] At the surface, however, dangling bonds can react to form native surface oxides.[3−6] Importantly, the oxides have been proposed to play an important role in controlling the electronic properties of buried device structures. For example, in power electronic devices, surface compensation can have a dramatic influence on the mobility of the two-dimensional electron gas (2DEG) that forms at AlGaN/GaN hetero-interfaces.[7−10]

Although further advancements require complete understanding of the native surface oxides, much remains unknown about their structure.[11−15] Methods such as X-ray photoelectron or Auger electron spectroscopies and electron diffraction provide key insights, but are an indirect probe. While scanning tunneling microscopy can probe the surface atomic and electronic structure, the outermost valence electrons are primarily probed. As a result, surface oxide structural models have thus largely relied on presumed atomic configurations paired with first-principles density functional theory (DFT) calculations to estimate relative stability of each model.[16] As a result, there are a number of competing surface oxide models that can be difficult or impossible to determine without direct surface and subsurface information from experiment.

Here, we report the direct observation of native oxides that form on III-nitride surfaces. Using aberration corrected scanning transmission electron microscopy (STEM) imaging and spectroscopy, the structure of these ultrathin oxides is directly determined for *c*-plane AlN and GaN surfaces. The observed oxides differ considerably from bulk structures, but with bonding configurations consistent with the corresponding group III oxide. Furthermore, these oxides are found to be more energetically stable than previous surface oxide models over a wide range of chemical environments. Finally, the potential impact of these structures' material growth and properties are also discussed.

After removing amorphous surface damage and contamination with hydrofluoric acid (HF) and subsequent exposure to air, atomic resolution annular dark-field (ADF) STEM reveals the formation of native surface layers on *c*-plane AlN and GaN (Figure 1). For both materials, the same ultra- thin, ∼ 0.6 nm layer structure is found across the c-plane surface. The layer is distinguished by a trilayer (dashed boxed regions) and a bilayer inverted relative to the substrate (solid boxes) as indicated in Figure 1A, B. Also, the orientation of the surface reverses 180°

Received: January 16, 2018
Accepted: March 20, 2018
Published: March 20, 2018

DOI: 10.1021/acsami.8b00845
ACS Appl. Mater. Interfaces 2018, 10, 10607−10611

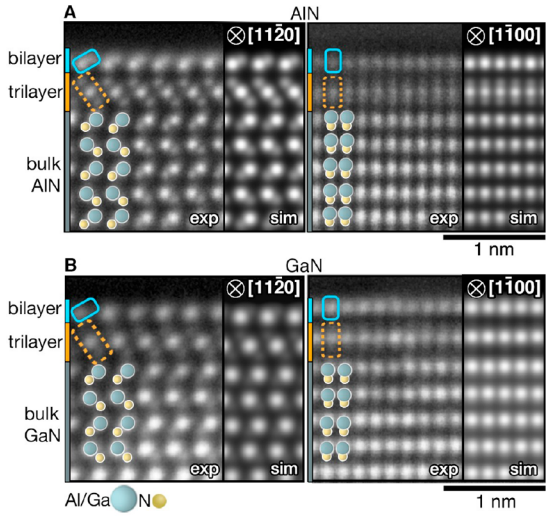

Figure 1. Ultrathin native oxides observed on the *c*-plane of (A) AlN and (B) GaN in ADF STEM experiments (exp). Perpendicular view directions are presented (left/right). The dashed (orange) and solid (blue) boxes highlight the trilayers and bilayers that comprise the oxide structure. Simulations (sim) are based on the model structure shown in Figure 3.

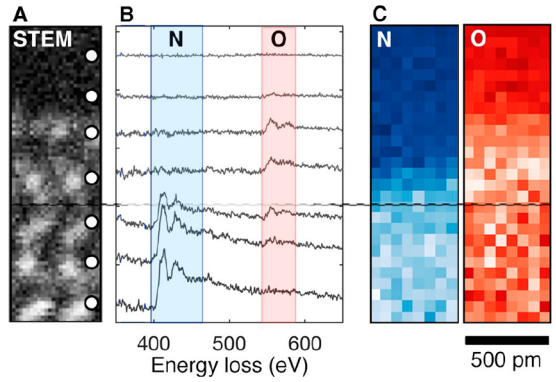

Figure 2. (A) ADF STEM and corresponding (B) integrated EEL spectra from across the *c*-plane AlN surface. Circles mark the approximate probe location. (C) Elemental distribution of the surface determined by background subtracting and integrating the spectral signal over the range indicated in B. The dashed line indicates the approximate oxide/nitride interface.

at nitride step edges, indicating a reduced symmetry relative to substrate (Figure S1). The outer surface is consistent with prior oxide formation studies using indirect methods and STM, but those methods could not resolve the subsurface information.[17] With regard to stability, the layered structure appears passivated as further growth of the oxide does not occur over time and was not noticeably modified during imaging with the electron beam.

Various TEM sample preparation approaches were attempted to rule out unintentional modification of the surface as outlined in the Supporting Information. Regardless of the preparation approach, the observed surface structure remained the same. While the results presented here are from HF etched samples, as-prepared electron microscopy samples show formation of the layer. In those cases, however, additional organic/inorganic contaminates and amorphous layers generated from ion milling prevented large area coverage of the native layer. Also, the use of etchants to prepare bare surfaces before exposure to air is consistent with prior studies of native oxide formation on III-nitride studies.[3]

Although atom column positions can be directly determined from the ADF STEM images, the atomic species can be difficult or impossible to identify without additional information.[18] For unambiguous elemental analysis, we turn to electron energy loss spectroscopy (EELS), where an abrupt transition from the nitride to a ultrathin oxide layer on AlN is seen in Figure 2. EELS of the GaN surface exhibits the same distribution of anions, as shown in Figure S2. It is important to note that only Ga/Al/O/N were detected with EELS and energy dispersive X-ray spectroscopy at or near the surface, and that oxygen is observed through the outermost layer. The oxygen signal is also found to extend into the nitride beyond the surface oxide, which indicates some oxygen−nitrogen intermixing within the first few layers of the wurtzite substrate surface. Combined with the oxide trilayer and bilayer, the total oxygen containing thickness is ∼1 nm for AlN and ∼2 nm for GaN, which is consistent with that of previous native oxide estimates based on indirect methods.[3−5]

Distance measurements from the perpendicular view directions in Figure 1 are used to construct a three-dimensional model of the oxides. Through use of revolving STEM,[19] accurate and precise[20] atom column distance measurements for AlN are included in Figure 3. The projected Al−N distances measured in the AlN substrate agree with those (expected) from bulk: 109 pm (107 pm) and 191 pm (192 pm). At the nitride/oxide interface, the first Al−O bond length is 176 pm. This length is consistent with the shorter bonds in bulk Al oxide, Al−O 175 pm,[21] than the nitrides. In the middle of the trilayer, the projected Al−O distance is 138 pm (Figure 3A,B). A comparison to GaN distance measurements is provided in Figure S3. In addition, in-plane distances between adjacent Al/Ga and N/O columns gradually decreases, as shown in Figure S4. To probe bond angles, the angle between neighboring anions on (0001) planes and the nearest group III atom column are measured, as shown for AlN in Figure 3C, D. The average angles are 34° and 48° for the AlN bulk and oxide, respectively. These are consistent the projected angles from AlN and Al_2O_3, which are 35 and 52°, respectively, where some deviation is expected due to strain in the surface oxide.

The structural measurements provide the parameters necessary to construct 3D models to determine the cation coordination in the oxide. First, the Ga and Al oxide cation layer at the oxide/nitride interface remains tetrahedrally coordinated with N at the base and O at the apex of the tetrahedron. Second, highly distorted cation−O octahedra are observed at the central oxide layer. This configuration appears encouraged by the tetrahedral coordination at the *c*-plane surface. Further, the relative fractions of tetrahedral and octahedral coordination in the surface structure are consistent with θ-Al_2O_3 and β-Ga_2O_3, as opposed to the other structural polymorphs.[22,22−26] Furthermore, this conclusion is consistent with that from indirect measurements suggesting the formation of β-Ga_2O_3 on GaN.[27] It is also noted in Figure 3E that there is an inversion of polarity across the midplane of the oxide trilayer based on this configuration, which suggests a role of these surface oxides in compensating the strong, built-in polarization field of the wurtzite nitride.

Though the oxidized surfaces of GaN and AlN have been studied and modeled for some time, the STEM results presented here reveal a new structure that differs from those previously investigated. To understand the energetic stability of

DOI: 10.1021/acsami.8b00845
ACS Appl. Mater. Interfaces 2018, 10, 10607−10611

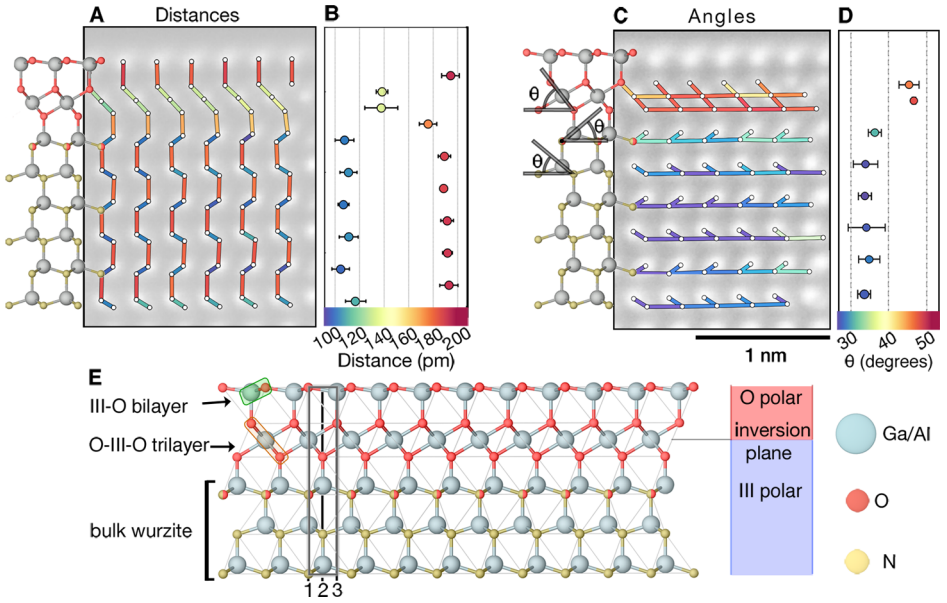

Figure 3. (A) Distances measured within the oxide and (B) corresponding layer averages. (C) Projected bond angle, θ, measured as depicted in the schematic and (D) corresponding layer averages. The color of each measurement corresponds to the relevant colorbar provided at the bottom. (E) Model of the AlN surface oxide constructed using the distance, angle, and chemical information from EELS.

this structure, we compare it with previously proposed models[16,17] using DFT. In those studies, it was found that the most energetically favorable structures consist of either an octahedrally coordinated O−III−O trilayer or a tetrahedrally coordinated III−O bilayer, which can be seen at the top of Figure 4. An ideal version of the observed structure maintains the bulk oxide 2/3 cation-to-anion ratio. This is achieved by combining aspects of both trilayer and bilayer models, which was not previously considered.

The surface formation energy for each configuration is calculated via eq 1. This surface energy is taken relative to a clean, smooth, and step-free cleaved nitride surface. Negative surface formation energies indicate that the oxidized configurations are favorable, for the particular set of conditions, relative to the unreconstructed and ideally flat surface. Absolute surface energies taken relative to the bulk are a challenge in this direction due to the lack of inversion symmetry along [0001]. Nevertheless, the relative energies provide insight into the favorability of one configuration as compared to another. The surface energy as a function of chemical potential is given by

$$E^{\mathrm{f}} = \frac{1}{A}\left[E^{\mathrm{tot}}_{\mathrm{slab}} - E^{\mathrm{tot}}_{\mathrm{ref}} - \sum_i n_i\mu_i\right] \quad (1)$$

In this equation, $E^{\mathrm{tot}}_{\mathrm{slab}}$ is the total energy of the slab model containing the reconstruction, $E^{\mathrm{tot}}_{\mathrm{ref}}$ is the energy of the eight bilayer reference, A is the area of the surface, n is the number of atoms added to (positive) or removed from (negative) the surface structure with atoms being exchanged with a chemical reservoir described by the chemical potential μ_i, where i is the element (Al, Ga, N, or O) being exchanged. The total chemical potential, μ_i, is $\mu_i = \mu_i^{\circ} + \Delta\mu_i$, where μ_i° is the reference chemical potential taken at 0 K and $\Delta\mu_i$ is the change in the chemical potential from that reference.

The calculated surface energies, E^{f}, as a function of the Al and Ga chemical potential for the observed structure and previously proposed models, are presented in Figure 4. Based on an environment of air with an oxygen partial pressure of 0.2 atm at room temperature (298 K), $\Delta\mu_{\mathrm{O}}$ is fixed at −0.3 eV.[28] Although previous studies showed that an oxide consisting of an O−Al−O trilayer is more energetically stable, the E^{f} calculated for the observed structure is yet still more favorable across the range of relevant Al and Ga chemical potentials.[16]

Using the relaxed DFT model based on the observed structure, STEM image simulations, Figure 1 (right panels), are in overall excellent agreement with the experiment. Although the STEM images from experiment shows that the oxide exhibits a slightly lower overall intensity compared to simulations, this can be due to either incomplete coverage of

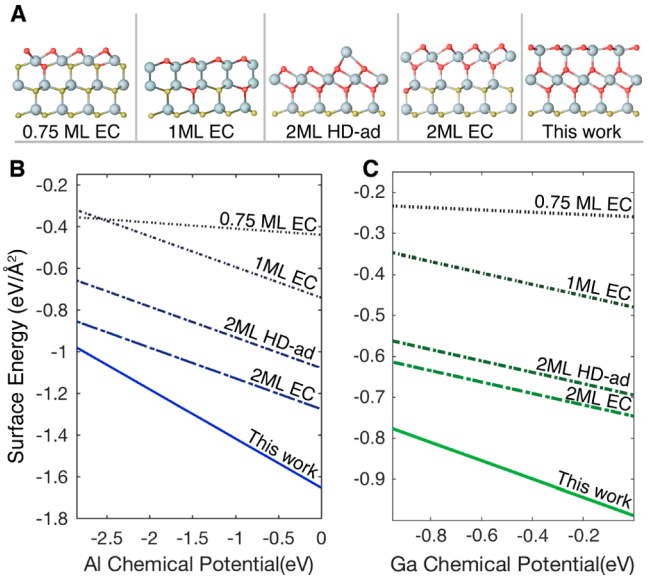

Figure 4. Surface formation energies for previously proposed oxide structures and the structure observed in this study. (A) Monolayer, high density, and adsorbed oxide models are indicated as ML, HD, and ad, respectively. Surface energies as a function of (B) Al and (C) Ga chemical potentials with an oxygen chemical potential of −0.3 eV.

DOI: 10.1021/acsami.8b00845
ACS Appl. Mater. Interfaces 2018, 10, 10607−10611

the oxide on the sample surface, differences in static and thermal atomic displacement factors, unoccupied cation sites, or a combination thereof. To further validate the surface oxide model, we compared the bond lengths and angles between experiment and DFT. The bond length measurements are shown in Table S1. The trends for each bond in and between the nitride and oxide are in excellent agreement. Quantitatively, the bond lengths exhibit at most ~5% error. The largest deviation occurs at the oxide/nitride interface. Further, the agreement extends to the bond angles, matching experiment and theory to within 0.5°.

Although calculating the complete range of all possible stability conditions (temperature, atmosphere, and pressure) is beyond the scope here, there are a number of these observations. First, inversion domain boundaries are often found in thin film nitrides,[29] and the observed oxides offer a mechanism for their creation. Notably, the oxides inherently reverse polarity through the transition from octahedral to tetrahedral bonding as discussed above. The inversion of polarity in the outermost layer of the oxide would seed N-polar nitride growth. Supporting this hypothesis, oxygen has been found at the initiation site of inverted domains, forming $AlN_{1-x}O_x$ at elevated growth temperatures.[29] Although the observed oxides and the $AlN_{1-x}O_x$ by Mohn et al. differ in structure, they consist of similar octahedral and tetrahedral bonding units. Differences between the two structures may result from reaction of the oxide seed layer during subsequent high temperature growth.

The structure of the observed oxide also provides insights into results from a recent study growing ZnO grown epitaxially on GaN. In that case, the surface of the GaN was intentionally oxidized before ZnO growth, where the ZnO polarity was then inverted.[30] The authors of that study hypothesized that a monolayer oxide was responsible for the polarity inversion and high quality of growth. The structural models provided here therefore provide critical insight into reducing defects as well as improved heteroepitaxial oxide−nitride thin film structures. A similar structure was also observed at the interface between an Al alloy and AlN after liquid phase bonding.[31] In that case, Mg−O octahedral cages form the central trilayer in contrast to the Al−O or Ga−O octahedra observed here. These oxides are also similar to the recently reported formation of a 2D form of GaN.[32] The structure, stabilized by encapsulation with graphene, also exhibits octahedral−tetrahedral bonding in a trilayer−bilayer configuration. In both cases, the polarity is inverted across the central trilayer, which could aid in charge compensation. As such, this structural configuration may be a hallmark of Ga- and Al-based 2D oxides and nitrides. Further, these similarities motivate future directions of research in the development of a mechanistic understanding of such ultrathin structures on polar surfaces and demonstrates that even though the nitrides have been studied for decades new discoveries remain.

In summary, by combining experiment and theory, we have directly solved the structure of ultrathin oxides forming natively on AlN and GaN surfaces. These oxide structures provide key observations to explain the formation of inversion domains and the origin of surface states that significantly influence the performance of III-nitride-based devices. Further, these models offer direct evidence to model electronic surface states within the bulk band structure. Because of the relative ease of forming these structures, we also propose that such a platform may provide opportunities for exploring the properties and electronic behavior of two-dimensional oxides not previously considered.

■ ASSOCIATED CONTENT

Supporting Information

The Supporting Information is available free of charge on the ACS Publications website at DOI: 10.1021/acsami.8b00845.

Materials & sample preparation, STEM experiment and simulation method details, DFT calculation method details, additional STEM images/spectroscopy (Figures S1−S4), and bond length measurements (Table S1) (PDF)

■ AUTHOR INFORMATION

Corresponding Author

*E-mail: jmlebeau@ncsu.edu.

ORCID

James M. LeBeau: 0000-0002-7726-3533

Notes

The authors declare no competing financial interest.

■ ACKNOWLEDGMENTS

J.M.L., J.H.D., and E.D.G. gratefully acknowledge support for this research from the Air Force Office of Scientific Research (FA9550-14-1-0182). D.L.I. and K.J.M. acknowledge financial support from the NSF (DMR-1151568). J.H.D. and E.D.G. acknowledge support by the National Science Foundation Graduate Research Fellowship (DGE-1252376). R.K., S.M., R.C., and Z.S. sincerely thank the NSF (ECCS-1508854, ECCS-1610992, DMR-1508191, ECCS-1653383) for the support, and the Army Research Office (W911NF-15-2-0068, W911NF-16-C-0101) for funding. This study was performed in part at the Analytical Instrumentation Facility (AIF) at North Carolina State University, which is supported by the State of North Carolina and the National Science Foundation (ECCS-1542015). AIF is a member of the North Carolina Research Triangle Nanotechnology Network (RTNN), a site in the National Nanotechnology Coordinated Infrastructure (NNCI).

■ REFERENCES

(1) Ibbetson, J. P.; Fini, P. T.; Ness, K. D.; DenBaars, S. P.; Speck, J. S.; Mishra, U. K. Polarization effects, surface states, and the source of electrons in AlGaN/GaN het- erostructure field effect transistors. *Appl. Phys. Lett.* **2000**, *77*, 250−252.

(2) Vetury, R.; Zhang, N. Q.; Keller, S.; Mishra, U. K. The impact of surface states on the DC and RF characteristics of AlGaN/GaN HFETs. *IEEE Trans. Electron Devices* **2001**, *48*, 560−566.

(3) Edwards, N.; Bremser, M.; Weeks, T., Jr.; Kern, R.; Davis, R.; Aspnes, D. E. Real-time assessment of overlayer removal on GaN, AlN, and AlGaN surfaces using spectroscopic ellipsometry. *Appl. Phys. Lett.* **1996**, *69*, 2065−2067.

(4) Lin, Y.-J.; Lin, W.-X.; Lee, C.-T.; Chang, H.-C. Electronic Transport and Schottky Barrier Heights of Ni/Au Contacts on n-Type GaN Surface with and without a Thin Native Oxide Layer. *Jpn. J. Appl. Phys.* **2006**, *45*, 2505−2508.

(5) Garcia, M. A.; Wolter, S. D.; Kim, T. H.; Choi, S.; Baier, J.; Brown, A.; Losurdo, M.; Bruno, G. Surface oxide relationships to band bending in GaN. *Appl. Phys. Lett.* **2006**, *88*, 013506.

(6) Prabhakaran, K.; Andersson, T. G.; Nozawa, K. Nature of native oxide on GaN surface and its reaction with Al. *Appl. Phys. Lett.* **1996**, *69*, 3212−3214.

(7) Shur, M.; Gelmont, B.; Asif Khan, M. Electron mobility in two-dimensional electron gas in AlGaN/GaN heterostructures and in bulk GaN. *J. Electron. Mater.* **1996**, *25*, 777−785.

DOI: 10.1021/acsami.8b00845
ACS Appl. Mater. Interfaces 2018, 10, 10607−10611

(8) Li, J. Z.; Lin, J. Y.; Jiang, H. X.; Khan, M. A.; Chen, Q. Two-dimensional electron gas in AlGaN/GaN heterostructures. *J. Vac. Sci. Technol., B: Microelectron. Process. Phenom.* **1997**, *15*, 1117−1120.
(9) Jogai, B. Influence of surface states on the two-dimensional electron gas in AlGaN/GaN heterojunction field-effect transistors. *J. Appl. Phys.* **2003**, *93*, 1631.
(10) Koley, G.; Spencer, M. G. On the origin of the two-dimensional electron gas at the AlGaNâĹŢGaN heterostructure interface. *Appl. Phys. Lett.* **2005**, *86*, 042107.
(11) Liao, H. M.; Sodhi, R. N. S.; Coyle, T. W. Surface composition of AlN powders stud- ied by x-ray photoelectron spectroscopy and bremsstrahlung-excited Auger electron spectroscopy. *J. Vac. Sci. Technol., A* **1993**, *11*, 2681−2686.
(12) Bermudez, V. M. Study of oxygen chemisorption on the GaN(0001)-(1 × 1) surface. *J. Appl. Phys.* **1996**, *80*, 1190−1200.
(13) Dalmau, R.; Collazo, R.; Mita, S.; Sitar, Z. X-ray photoelectron spectroscopy charac- terization of aluminum nitride surface oxides: thermal and hydrothermal evolution. *J. Electron. Mater.* **2007**, *36*, 414−419.
(14) Li, J.; Nakamura, M.; Shirai, T.; Matsumaru, K.; Ishizaki, C.; Ishizaki, K. Mechanism and kinetics of aluminum nitride powder degradation in moist air. *J. Am. Ceram. Soc.* **2006**, *89*, 937−943.
(15) Rice, A.; Collazo, R.; Tweedie, J.; Dalmau, R.; Mita, S.; Xie, J.; Sitar, Z. Surface preparation and homoepitaxial deposition of AlN on (0001)-oriented AlN substrates by metalorganic chemical vapor deposition. *J. Appl. Phys.* **2010**, *108*, 043510.
(16) Miao, M. S.; Weber, J. R.; Van de Walle, C. G. Oxidation and the origin of the two- dimensional electron gas in AlGaN/GaN heterostructures. *J. Appl. Phys.* **2010**, *107*, 123713.
(17) Dong, Y.; Feenstra, R. M.; Northrup, J. E. Oxidized GaN(0001) surfaces studied by scanning tunneling microscopy and spectroscopy and by first-principles theory. *J. Vac. Sci. Technol. B Microelectron. Nanom. Struct.* **2006**, *24*, 2080.
(18) Houston Dycus, J.; White, R. M.; Pierce, J. M.; Venkatasubramanian, R.; LeBeau, J. M. Atomic scale structure and chemistry of Bi_2Te_3/GaAs interfaces grown by metallorganic van der Waals epitaxy. *Appl. Phys. Lett.* **2013**, *102*, 081601.
(19) Sang, X.; LeBeau, J. M. Revolving scanning transmission electron microscopy: Cor- recting sample drift distortion without prior knowledge. *Ultramicroscopy* **2014**, *138*, 28−35.
(20) Dycus, J. H.; Harris, J. S.; Sang, X.; Fancher, C. M.; Findlay, S. D.; Oni, A. A.; Chan, T.-t. E.; Koch, C. C.; Jones, J. L.; Allen, L. J.; Irving, D. L.; LeBeau, J. M. Accurate nanoscale crystallography in real-space using scanning transmission electron microscopy. *Microsc. Microanal.* **2015**, *21*, 946−952.
(21) Jones, J. B. Al−O and Si−O tetrahedral distances in aluminosilicate framework struc- tures. *Acta Crystallogr., Sect. B: Struct. Crystallogr. Cryst. Chem.* **1968**, *24*, 355−358.
(22) Zhou, R.-S.; Snyder, R. L. Structures and transformation mechanisms of the η, γ and θ transition aluminas. *Acta Crystallogr., Sect. B: Struct. Sci.* **1991**, *47*, 617−630.
(23) Kovarik, L.; Bowden, M.; Genc, A.; Szanyi, J.; Peden, C. H. F.; Kwak, J. H. Structure of δ-alumina: Toward the atomic level understanding of transition alumina phases. *J. Phys. Chem. C* **2014**, *118*, 18051−18058.
(24) Lee, M.-H.; Cheng, C.-F.; Heine, V.; Klinowski, J. Distribution of tetrahedral and octahedral A1 sites in gamma alumina. *Chem. Phys. Lett.* **1997**, *265*, 673−676.
(25) Playford, H. Y.; Hannon, A. C.; Barney, E. R.; Walton, R. I. Structures of uncharac- terised polymorphs of gallium oxide from total neutron diffraction. *Chem. - Eur. J.* **2013**, *19*, 2803−2813.
(26) Irokawa, Y.; Suzuki, T. T.; Yuge, K.; Ohi, A.; Nabatame, T.; Kimoto, K.; Ohnishi, T.; Mitsuishi, K.; Koide, Y. Low-energy ion scattering spectroscopy and reflection high- energy electron diffraction of native oxides on GaN(0001). *Jpn. J. Appl. Phys.* **2017**, *56*, 128004.
(27) Wolter, S. D.; Mohney, S. E.; Venugopalan, H.; Wickenden, A. E.; Koleske, D. D. Kinetic study of the oxidation of gallium nitride in dry air. *J. Electrochem. Soc.* **1998**, *145*, 629−632.
(28) Mallard, W. G., Linstrom, P. J., Eds. *NIST Chemistry WebBook, NIST Standard Reference Database Number 69*; National Institute of Standards and Technology:Gaithersburg, MD, 2009.
(29) Mohn, S.; Stolyarchuk, N.; Markurt, T.; Kirste, R.; Hoffmann, M. P.; Collazo, R.; Courville, A.; Di Felice, R.; Sitar, Z.; Vennéguès, P.; Albrecht, M. Polarity Control in Group-III Nitrides beyond Pragmatism. *Phys. Rev. Appl.* **2016**, *5*, 54004.
(30) Ullah, M. B.; Avrutin, V.; Li, S. Q.; Das, S.; Monavarian, M.; Toporkov, M.; Özgür, Ü.; Ruterana, P.; Morkoç, H. Polarity control and residual strain in ZnO epilayers grown by molecular beam epitaxy on (0001) GaN/sapphire. *Phys. Status Solidi RRL* **2016**, *10*, 682−686.
(31) Kumamoto, A.; Shibata, N.; Nayuki, K.-i.; Tohei, T.; Terasaki, N.; Nagatomo, Y.; Nagase, T.; Akiyama, K.; Kuromitsu, Y.; Ikuhara, Y. Atomic structures of a liquid- phase bonded metal/nitride heterointerface. *Sci. Rep.* **2016**, *6*, 22936.
(32) Al Balushi, Z. Y.; Wang, K.; Ghosh, R. K.; Vilá, R. A.; Eichfeld, S. M.; Caldwell, J. D.; Qin, X.; Lin, Y.-C.; DeSario, P. A.; Stone, G.; Subramanian, S.; Paul, D. F.; Wal- lace, R. M.; Datta, S.; Redwing, J. M.; Robinson, J. A. Two-dimensional gallium nitride realized via graphene encapsulation. *Nat. Mater.* **2016**, *15*, 1166−1171.

DOI: 10.1021/acsami.8b00845
ACS Appl. Mater. Interfaces 2018, 10, 10607−10611